

The Effect of Laser Irradiation on The Properties of Micro to Nanolayer Titanium Alloy

Hebatalrahman¹

¹ Dr. Eng Consultant in Material Science, Cairo, Egypt

Correspondence: Hebatalrahman, Dr. Eng Consultant in Material Science, Cairo, Egypt. E-mail: hebatalrahman11@yahoo.com, hebatalrahman11@gmail.com

Received: October 12, 2022 Accepted: November 14, 2022 Online Published: January 30, 2023

doi:10.5539/jmsr.v11n2p11

URL: <https://doi.org/10.5539/jmsr.v11n2p11>

Abstract

In this work, a new technique for Laser irradiation of Ti6Al4VELI was developed, this alloy is an alpha-beta structure, the irradiation was done at room temperature in the normal atmosphere without any external media, the effects of laser irradiation on the Ti6Al4VELI such as the chemical composition of the alloy before and after laser irradiation were recorded by Energy dispersive X-ray “EDX” technique. the affected zone (thickness) of the laser irradiation technique was limited to the surface in micro to the nanoscale. The variation in mechanical properties due to laser irradiation at different wavelengths was measured by the determination of the variation of modulus and hardness at maximum load with a number of pulses. The wear rate was measured for the Ti6Al4VELI before and after laser irradiation at 5000 pulses where the maximum improvement in the hardness occurs at all wavelengths, in the current study, it improves surface mechanical characteristics. The effect of laser irradiation on the structures was studied by SEM, the quantitative analysis was done at all irradiation conditions. Laser treatment is suitable for both field works and industry. The improvement in mechanical properties occurs due to microstructure changes without significant changes in chemical composition. the efficiency and lifetime of the alloys were increased, the work is registered as patent number 24014 in the Egyptian patent office.

Keywords: laser, irradiation, nanolayer, wear, surface treatment, titanium

1. Introduction – State of Art

Titanium can exist in two crystal forms. The first is alpha, which has a hexagonal close-packed crystal structure, and the second is beta, which has a body-centered cubic structure (Hebatalrahman, 2019; Saaïd et al., 2020). In unalloyed titanium, the alpha phase is stable at all temperatures up to 1620 °F (880 °C.) where it transforms to the beta phase. This temperature is known as the beta transus temperature. The beta phase is stable from 1620 °F (880 °C.) to the melting point (Rossetto Gilberto et al., 2013).

As alloying elements are added to pure titanium, the elements tend to change the temperature at which the phase transformation occurs and the amount of each phase present (Hebatalrahman, 2012). Alloy additions to titanium, except tin and zirconium, tend to stabilize either the alpha or the beta phase. Elements called alpha stabilizers stabilize the alpha phase to higher temperatures and beta stabilizers stabilize the beta phase to lower temperatures (Hebatalrahman 2016; Ardelean et al., 2016). The classification of titanium according to chemical composition means studying the effect of alloying elements on the microstructure (Ardelean et al., 2016; Hebatalrahman, 2014). Alloying elements generally can be classified as α and β stabilizers. Alpha stabilizers such as Aluminium and oxygen, increase the temperature at which the α phase is stable. Beta stabilizers such as Vanadium and Molybdenum, result in instability of the β phase at lower temperatures. This transformation temperature from $\alpha + \beta$ or from α to all β is known as the β transus temperature. The β transus is defined as the lowest equilibrium temperature at which the material is 100% β (Zhou et al., 2021; Bhardwaj et al., 2019). The β transus is critical in deformation processing and heat treatment. Below the beta β transus temperature, Titanium is a mixture of $\alpha + \beta$ if the material contains some β stabilizers; otherwise, it is all α if it contains limited or no β stabilizers (Moridi et al., 2019; Aboulkhair et al., 2019). The β transus is important. Because processing and heat treatment often is carried out with reference to some incremental temperature above or below the β transus. Alloying elements that favor the α crystal structure and stabilize it by raising the β transus temperature include Aluminium, gallium, Germanium, Carbon, Oxygen, and Nitrogen (Lu et al., 2021; Marchese et al., 2018).

High strength alloys: Ti-6Al-4V Grade 5 is the black horse alloy in various engineering applications due to its light weight and high durability, this alpha-beta alloy is the workhorse alloy of the titanium industry (Y. Xu et al, 2020; Zhang et al., 2019). The alloy is fully heat-treatable in section sizes up to one inch and is used up to approximately 400 °C (750 °F). Since it is the most commonly used alloy - over 70% of all alloy grades melted are a sub-grade of Ti-6Al-4V - its uses span many aerospace engine and airframe components uses and also major non-aerospace applications in the marine, offshore and power generation industries in particular (Wei et al., 2020).

The addition of 0.05% palladium, (Grade 24), 0.1% ruthenium (Grade 29) and .05% palladium and 0.5% nickel (Grade 25) significantly increases corrosion resistance in reducing acid chloride and sour environments, raising the threshold temperature for attack to well over 200 °C (392 °F). Ti-6Al-4V ELI (Grade 23). The essential difference between Ti-6Al-4V ELI (Grade 23) and Ti-6Al-4V (Grade 5) is the reduction of oxygen content to 0.13% max in Grade 23. This confers improved ductility and fracture toughness, with some reduction in strength. Grade 23 has been widely used in fracture critical airframe structures and for offshore tubular (Donachie, 2000). Mechanical properties for fracture critical applications can be enhanced through processing and heat treatment. Grade 29 also having a lowered level of oxygen will deliver similar levels of mechanical properties to Grade 23 according to processing. Grade 23 was used in our study and irradiated by lasers in the normal atmosphere, figure 1 shows the Phase diagram and crystal structure of Ti6Al4VELI (Zhao et al., 2016; Selvaganesh et al., 2021).

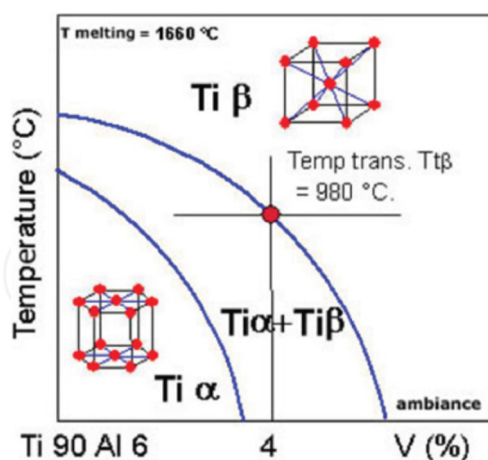


Figure 1. Phase diagram and crystal structure of Ti6Al4VELI

2. Experimental Work

2.1 Materials

The alloys used throughout this work were supplied by Sandvik Co, France in the form of bars of Ti6Al4VELI. Table (1) shows the chemical composition of the alloy used Table (1) the chemical composition of Ti6Al4VELI (grade 23)

Table 1. The chemical composition of Ti6Al4VELI (grade 23)

Elements	Symbol	Percent %
Carbon(maximum)	C	0.08%
Aluminium	Al	5.5%:6.5%
Nitrogen(maximum)	N	0.05%
Oxygen(maximum)	O	0.130%
Vanadium	V	3.5:4.5%
Iron(maximum)	Fe	0.25%
Hydrogen(maximum)	H	0.013%
Yttrium	Y	0.005%
Titanium	Ti	Balance
Others traces (maximum)	-	0.04%

2.2 Laser Surface Irradiation

The surface irradiation of the alloys was studied. Samples used in this investigation were in the standard size for every test according to ASTM. All the experiments were performed at room temperature in air at atmospheric pressure; it was shown elsewhere (Zhou et al., 2021) that the presence of air has no measurable influence on the process of irradiation by UV laser (Bhardwaj et al., 2019). The irradiation is done on one side of the sample and covers all the surface area of the sample. The main goal of this work is an optimized condition for laser irradiation of the samples by Excimer laser at 308nm Table (3) shows data for used rare gas halide Excimer laser.

Table 2. Data for Excimer Laser (rare gas halide)

Gas type	(nm)	r(A)	(cm ⁻¹)	(cm ²)	(ns)
XeCl	308	2.9	194	50	11
Arf	193	2.2	-	12	4.2

λ =transition wavelength

$r(A)$ =equilibrium inter-nuclear separation

ω = fundamental vibration frequency of the excited state

σ = stimulated emission cross section

τ = radiative life time (pulse duration)

The number of pulses and the effect of energy per pulse on the hardness were recorded to indicate the energy required (fluence) to improve the mechanical properties. In the shape of a rectangle with width (w=4mm) and length (l=10mm) was used in the laser process the power density ranges from (0.75 W/Cm² to 0.1 W/Cm²) without any focusing. The laser irradiation condition is listed in Table (3)

Table 3. Laser Irradiation Conditions

Type	Wavelength nm	Number of pulses	Energy per pulse mJ	Repetition rate Hz	Time Nano-second
Excimer UV	308.6	0	6	200	6
		2000			
		5000			
		10250			
		15000			
		50000			
Excimer UV	193	0	6	200	6
		2000			
		5000			
		10250			
		15000			
		50000			

$$\text{Total energy} = \text{energy per pulse} \times \text{number of pulses} \quad (1)$$

Excimer laser irradiation is performed directly in the air and without any intermediate media, figure (2) shows a schematic presentation of the laser irradiation process.

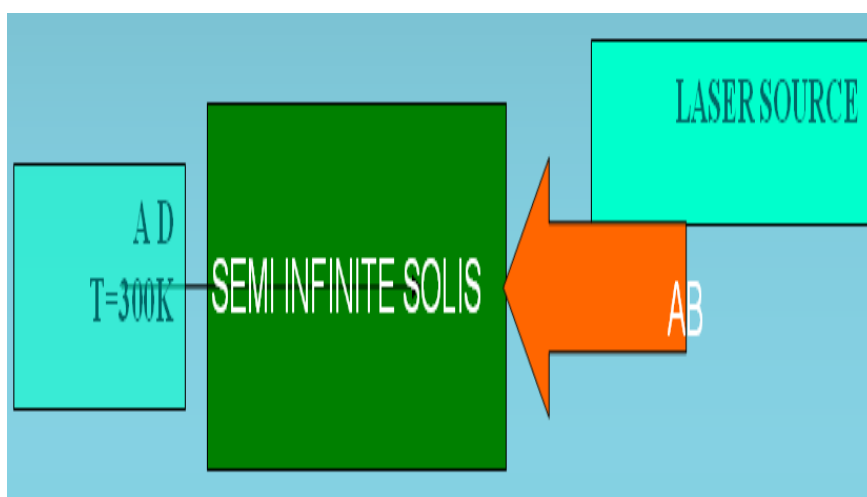


Figure 2. schematic presentation of the laser irradiation process

2.3 Energy-Dispersive X-ray “EDX”

The quantitative method of elemental analysis of the samples has been examined at the Chemical labs of the ministry of Telecommunication in Egypt by SEM JSM-T200 at 25KV acceleration voltage, 20mm working distance, and magnification 200x, (1peak omitted 0.02 KeV). Each value is at least an average of 2 readings

2.4 Mechanical Measurements

2.4.1 Superficial Hardness

The hardness of the specimens was measured at the Mechanical Engineering department at AUC by using a Superficial Rockwell hardness tester with ball diameter 1/16" at load 30 Kg. Each hardness value is at least an average of 5 readings and they are good to $\pm 4\%$.

2.4.2 Wear and Friction Coefficient

A pin-on-disk wear test (ASTM G 99) was selected to measure the wear before and after laser irradiation at El-Nasr Automotive Co in Egypt. A pin with a round tip is positioned perpendicular to a flat disk. A ball, rigidly held is often used as the pin specimen. The test machine rotates the disk at 60 to 600 rpm. The wear path is a circle on the disk surface. Surface finishes of 32 μin (AA) or less are typically used. Test results are usually reported as volume loss per cubic millimeter for the pin. The test has been done under load of 1Kg. Each value is at least an average of 3 readings.

2.5 Scanning Electron Microscope (SEM)

The specimens were examined by scanning electron microscope (SEM) operating at a nominal accelerating voltage of 30kv. Specimen preparation is very simply accomplished by cutting a thin slice of the specimen containing the surface of interest, chemical and electrostatic etching was done the specimens fixed on metallic holder (Cu) for dirt examination of the laser irradiation effects on the structure.

2.6 Quantitative Metallography Measurements

A quantitative analysis of the microstructures was produced carried out over four (4) fields across the surface to indicate:

- 1) The volume fraction V_f of each phase (count analysis was applied).
- 2) Average grain size by linear intercept technique.
- 3) Average particles radius D_A using number of modules per un area and can be calculated as follows:

$$D_A = \left(\frac{4V_f}{N_g} \right)^{1/2} \quad (2)$$

V_f volume fraction of secondary phase

N_g average grain size number

D_A Average particles radius

3. Results and Discussion

3.1 Energy-Dispersive X-ray "EDX"

To study the effect of laser irradiation on the Ti6Al4VELI the chemical composition of the alloy before and after laser irradiation were recorded by the Energy-dispersive X-ray "EDX" technique. Table (4) shows EDX analysis of Ti6Al4VEL samples before and after laser irradiation at optimum conditions, change in chemical composition due to laser irradiation is relatively very small and the slight change in the chemical composition does not affect the properties. Figure (3-a) and figure (3-b) show the spectrum of EDX analysis; the distribution is relatively unchanged in the case of Ti6Al4VELI. The slight change in some elements is due to the diffusion of some elements in the solid state as a result of laser irradiation and the formation of new microstructures. In general laser irradiation does not produce any significant effect in the elemental distribution and no reasonable change in the chemical composition but some elements such as Ba (barium) may immigrate due to diffusion of elements resulting from the ability of this element to absorb laser irradiation at specified wavelengths (Zhou et al,2021).

Table 4. EDX analysis of Ti6Al4VEL samples before and after laser irradiation at optimum conditions

Element	Before laser irradiation		After laser irradiation	
	Element	Atomic	Element	Atomic
	%	%	%	%
Ti	72.31	80.53	72.61	80.55
Al	3.52	6.96	3.53	6.94
V	4.75	4.97	4.99	5.21
Ba	19.43	7.55	18.87	7.30

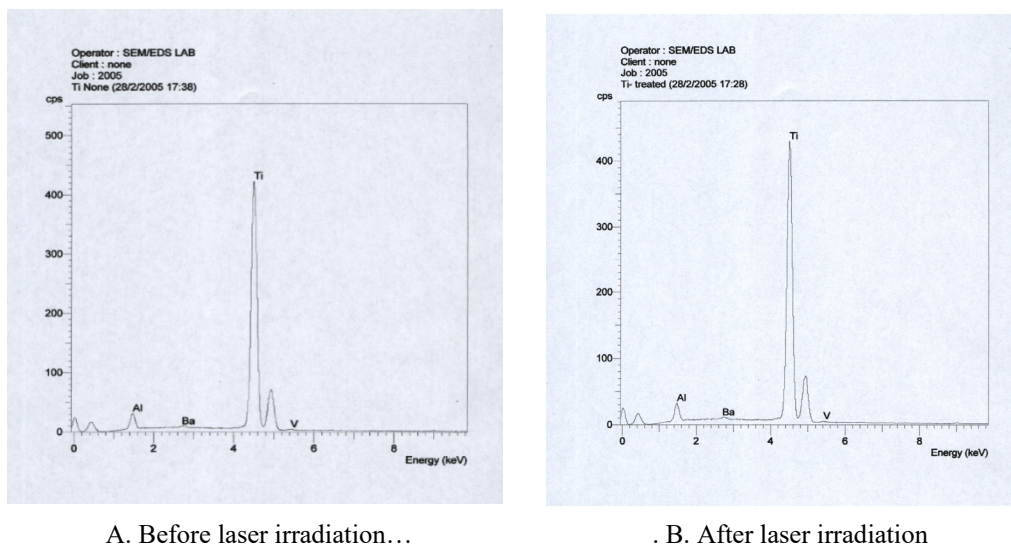


Figure 3. EDX Energy dispersive x-ray of Ti6Al4VELI

3.2 Mechanical Tests

3.2.1 Hardness

The variation in mechanical properties due to laser irradiation at different wavelengths was measured. Figure (1) and Figure (2) show the variation of modulus and hardness at maximum load with the number of pulses,

Figure (4) shows the variation of Hardness at maximum load with the number of pulses at 308nm, the value of modulus increased until 5000 pulses. The decreasing rate in modulus after 5000 pulses has sinusoidal behavior while remaining constant when the number of pulses was more than 10250 pulses.

The variation of hardness at maximum load with the number of pulses at 193nm laser irradiation was shown in Fig (5). The hardness value increases slightly to reach its maximum value in the range between 5000 and 10250 pulses after that the hardness was decreased slightly with the increase in the number of pulses.

When the number of pulses increased the hardness value decreased due to sample burning. The effect of the number of laser pulses on the hardness of **Ti6Al4VELI** was irradiated at 193nm and 308nm have almost similar behavior. The beam energy at 193nm pulses is larger than the beam energy at 308nm. According to the energy equations and principles, low wavelengths mean higher frequency and higher amount of energy absorbed. The improvement at 308nm is better in some points due to changes in the grain size and distribution of $\alpha + \beta$ structure which will be explained in terms of microstructure change. The initial microstructure of the irradiated alloy (the room temperature microstructure) plays a significant role in that case. The decrease in hardness of **Ti6Al4VELI** after laser irradiation is due to the formation of higher energy phases but these phases have a lower hardness.

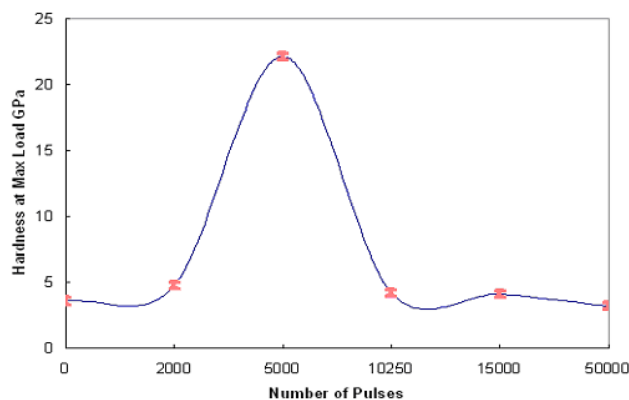


Figure 4. The variation of hardness at Maximum load with the number of pulses for Ti6Al4VELI irradiated with Excimer laser at 308 nm, 200 Hz, 6 mJ

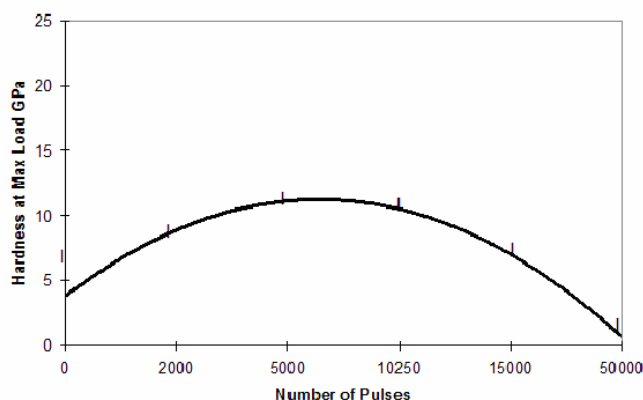


Figure 5. The variation of hardness at Maximum load with the number of pulses for Ti6Al4VELI irradiated with Excimer laser at 193 nm, 200 Hz, 6 mJ

3.2.2 Wear Resistances

The wear rate was measured for the **Ti6Al4VELI** before and after laser irradiation at 5000 pulses where the maximum improvement in the hardness occur at all wavelengths in the current study. Increasing the surface load between sliding surfaces has been found to cause a proportional increase in material wear rates.

Increasing the sliding distance of an assembly will cause a roughly proportional increase in material loss. Table (4) shows wear variation at constant test conditions and the effect of laser irradiation on the wear resistance improvements.

Wear resistance generally increases proportionally with increasing surface hardness (which may be very different from bulk hardness). Surface deformation during wear causes a localized increase in surface hardness on work-hardened metals. This explains why the irradiated **Ti6Al4VELI** are more wear resistant than un-irradiated **Ti6Al4VELI**.

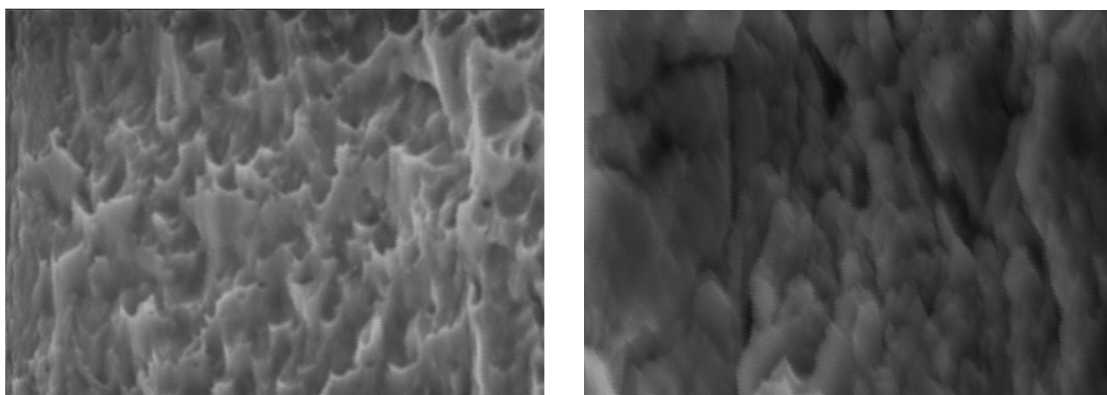
Very smooth surfaces promote cold welding (galling) because of high molecular interaction. High finishes also lack adequate clearance to store wear debris. Overly rough finishes increase wear by allowing surface asperities (irregularities) to become interlocked, resulting in what is known as a "stick-slip" phenomenon as these surface irregularities are subsequently worn off when sliding occurs.

Table 4. The improvement in wear characteristics for Ti6Al4VELI before and after laser irradiation

Material	Units	Before irradiation	After irradiation
Weight before	W(gm)	77.52	77.5
Weight after	W(gm)	77.5	77.7
Weight difference	W(gm)	0.02	0
Wear volume	cm ³	0.004165	0
Wear coefficient		43.9804	0
Wear rate	Cm ³ /mm	2.0835E-7	0
Improvement %	%	100	

3.3 Scanning Electron Microscope (SEM)

The effect of laser irradiation on the structures was studied by SEM before and after irradiations at 5000 pulses because these values introduce significant improvement in properties. Fig (6) shows SEM of **Ti6Al4VELI** at 2000X before and after laser irradiation by Excimer laser 308nm, 200Hz, 5000 pulses, 6 mJ, (a) Before irradiation and (b) After irradiation, the qualitative analysis of the samples show significant increase in the grain size due to laser irradiation.



A. Before laser irradiation

B. After Laser irradiation

Figure 6. SEM of Ti6Al4VELI at 2000X before and after laser irradiation by Excimer laser 308 nm, 200 Hz, 5000 pulses, 6 mJ

Qualitative analysis for the samples grain size at all number of pulses in the study range, all micro grain size measurements were calculated according to ASTM standard, grain size number, average diameter of the grain, average intercept distance, average number of the grains per unit and average number of the grains per unit volume and nominal grain at standard magnification were evaluated before and after laser irradiation at different number of pulses as shown in table (5).

3.4 Quantitative Analysis

The relation between the grain size number and average grain diameter as function of the number of pulses were plotted in figure (7) and (8) respectively. the grain size number decreased while average grain size increased gradually with increase in the amount of laser energy photons absorbed and reach maximum size of the grains at 5000 pulses, when the number of pulses increased over 5000 pulses the average grain size decreased due to the effect of secondary phase as shown in figure (1). β phase have BCC structure and less grain size than α structure which is HCP structure.

Table 5. The qualitative analysis of samples before and after laser irradiation

Micro-grain size measurements	Before irradiation	After irradiation				
		2000 pulses	5000 pulses	15000 pulses	10250 pulses	50000 pulses
ASTM grain size number	10	9.5	7.5	10	10	10
Diameter of average grain μm	11	13	27	11	11	11
Average intercept distance μm	10	11.9	23.8	10	10	10
Area of average grain section $\text{mm}^2 \times 10^{-6}$	126	178	0.713×10^{-3}	126	126	126
Average number of grains per unit volume $\text{mm}^3 \times 10^{-6}$	0.566	0.336	0.029630	0.566	0.566	0.566
Nominal grain per unit area mm^2	7940	5610	1111	7940	7940	7940
Nominal grain per mm^2 at 100x	512-645	362	71-68	512-645	512-645	512-645

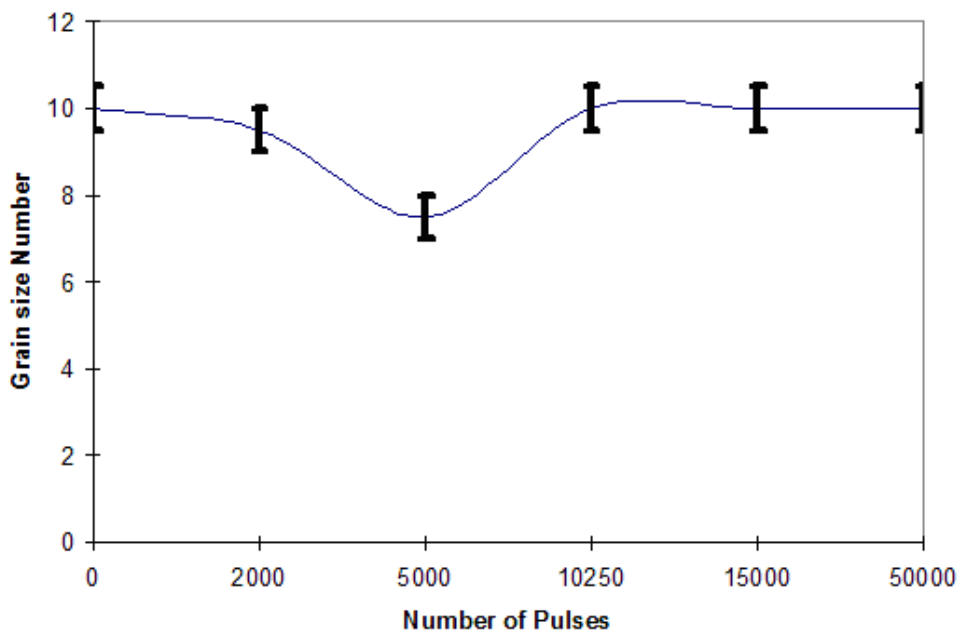


Figure 7. The relation between the number of pulses and grain size number for Ti6Al4VELI irradiated with Excimer laser at 308nm ,200Hz,6mJ.

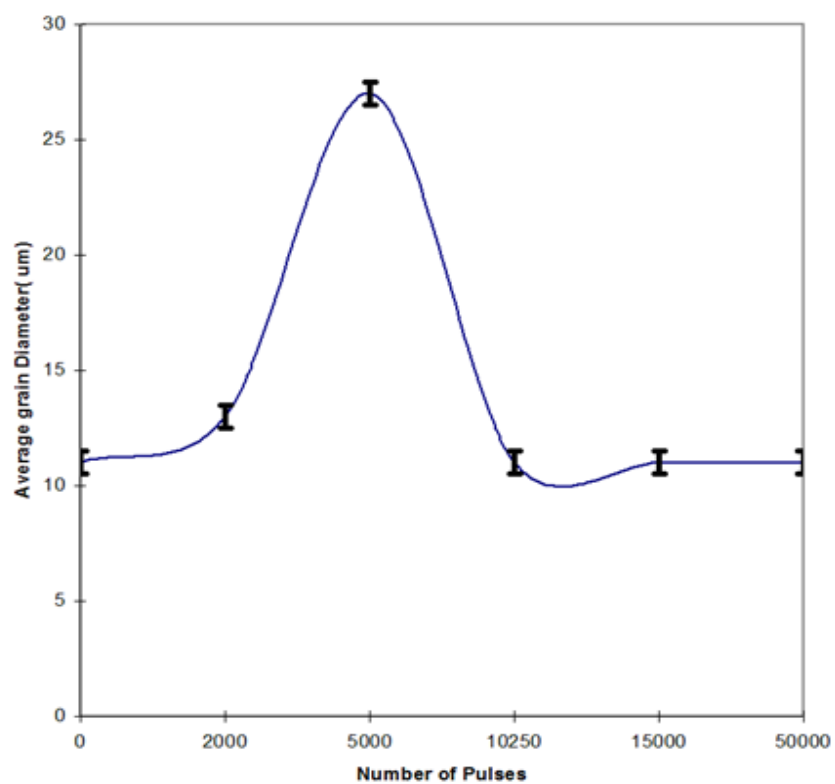


Figure 8. The relation between the number of pulses and grain size number for Ti6Al4VELI irradiated with Excimer laser at 193nm ,200Hz,6mJ.

3.5 Comparing Laser Treatment with Conventional Methods

Commercially pure titanium and many alloys generally have a limited response to heat treatment and work hardening; strength and surface hardness can be obtained from the heat treatable meta-stable beta alloys but compressive surface treatment such as solution treated, annealing and aging is normally beneficial, but surface treatment is normally beneficial for the various reasons given over, Table (6) indicates the extent to which typical alloy Ti6Al4VELI will respond to heat treatment.

Table 6. The treatment of Ti6Al4V Grade 5 by conventional methods

Alloy	Heat treatment	Annealed or Solution treated (hardness HV)	Heat treated and aged (hardness HV)	Comment
Grade 5	750 °C 1hr WQ	275-300	350-40	Limited in effect with sections above 20mm
Ti6Al4V	500 °C 2hr AC			

Ti6Al4VELI is the black horse alloy in the modern engineering industries, the major advantages of laser surface hardening include close control of the power input compared with conventional methods; the high-power density provided by the laser, which in turn maximize the total energy input and, the ability of the laser to reach normally inaccessible areas on the work-piece surface. Because no vacuum or protective atmosphere enclosure is needed, and because the distance from the workpiece to the last optical element of the laser system can be quite long. It is possible to process very large or irregular-shaped workpieces.

4. Conclusion

- 1) The main idea of the new method depends on the laser photon energy which is absorbed by the samples and causes microstructure changes leading to improvement in the mechanical properties without any significant changes in chemical composition.
- 2) Properties of the treated **Ti6Al4VELI** alloys was recorded to bimproved hardness by 36% (the hardness improved from 318 MHV to 437 MHV) – wear is improved by 99.8%- the particle size change from 10 to 7.5 ASTM - thickness of the treated part is only 250 nm.
- 3) Improving the mechanical properties of the **Ti6Al4VELI** alloys such as hardness and wear,increasing the efficiency of operation and lifetime is very important to improve economic feasibility.
- 4) Extends the lifetime of the alloys and makes them suitable for many applications such as bone replacement parts, dental elements, space applications, marine applications, industrial spare parts and increases the efficiency of surgical instruments.
- 5) The new treatment method makes **Ti6Al4VELI** alloys suitable for Applications that require long periods of operation and maintain the dimensions stability.
- 6) Ti6Al4V is the black horse alloy in various engineering applications due to its lightweight and high durability, the new method is addressing of the alloys and overcomes the problems of relatively high prices.
- 7) The new laser treatment technique has the following industrial features compared with conventional methods: -processing is performed directly in the air and without any intermediate liquid or gas.
 - A. New method does not use expensive chemicals such as surface coverage.
 - B. New methods do not include any complex interactions, hazardous wastes or harmful gases that may affect the environment.
 - C. User's treatment process is relatively economic. It does not need huge industrial equipment in a great place for the installation and operation of such equipment.
 - D. The main components in the new method are only the laser source and optical parts, it is considered as the only surface treatment method is done in the field.

5. Recommendation for Future Work

The different grades of titanium alloys such as grade 29, grade 5, and so on will be irradiated and tested at the same conditions, besides the other nonferrous alloys and ferrous alloys.

References

- Aboulkhair, N. T., Simonelli, M., Parry, L., Ashcroft, I., Tuck, C., & Hague, R. (2019). 3D printing of Aluminium alloys: Additive Manufacturing of Aluminium alloys using selective laser melting. *Progress in materials science*, 106, 100578. <https://doi.org/10.1016/j.pmatsci.2019.100578>
- Ahmed, H. (2010). Nano indentation effects on SS 316L during excimer laser irradiation. *Journal of Physics*, 1, 34-39.
- Ahmed, H. (2010). Nano indentation effects on SS 316L during excimer laser irradiation. *Journal of Physics*, 1, 34-39.
- Ahmed, H. (2019, April). Factors affecting irradiation of nano & micro materials by laser treatment industrial unit. In *International Conference on Aerospace Sciences and Aviation Technology* (Vol. 18, No. 18, pp. 1-11). The Military Technical College. <https://doi.org/10.1088/1757-899X/610/1/012005>
- Ardelean, J. et al. (2016). Investigations on Dental Alloys Using Metallographic Observation, Scanning Electron Microscopy, and Energy-Dispersive X-Ray Spectroscopy In: Stefan G. Stanciu, editor. *Micro and Nanotechnologies for Biotechnology: InTech*, 123-143. <https://doi.org/10.5772/61530>
- Ardelean, J. et al. (2016). *Superalloys for Industry Applications the world's leading publisher of Open Access books*. Retrieved from www.intechopen.com
- Bhardwaj, T., Shukla, M., Paul, C. P., & Bindra, K. S. (2019). Direct energy deposition-laser additive manufacturing of titanium-molybdenum alloy: Parametric studies, microstructure and mechanical properties. *Journal of Alloys and Compounds*, 787, 1238-1248. <https://doi.org/10.1016/j.jallcom.2019.02.121>
- Donachie, M. J. (2000). *Titanium: a technical guide*. ASM international. <https://doi.org/10.31399/asm.tb.ttg2.9781627082693>
- Ge, P., Zhang, Z., Tan, Z. J., Hu, C. P., Zhao, G. Z., & Guo, X. (2019). An integrated modeling of process-structure-property relationship in laser additive manufacturing of duplex titanium alloy. *International Journal of Thermal Sciences*, 140, 329-343. <https://doi.org/10.1016/j.ijthermalsci.2019.03.013>
- Hebatalrahman, A., Rossetto, G., & Carta, G. (2013). Nano Indentation Effects of XeCl pretreatment of The Alumina Coated on AISI 304. *The 1st International Engineering Conference Hosting Major International Events: Innovation Creativity & Impact Assessment Cairo Egypt*, 15-18 January 2013.
- Hebatalrahman, H. (2016, April). Laser Indirect Exposure Method for Treatment of Nanomaterials. In *The International Conference on Electrical Engineering* (Vol. 10, No. 10th International Conference on Electrical Engineering ICEENG 2016, pp. 1-13). Military Technical College. <https://doi.org/10.21608/iceeng.2016.30350>
- Hebatalrahman, H. A., & Zaki, S. I. (2020). Measurements & Detection Techniques in Nanotechnology in Road Applications. *World Journal of Nano Science and Engineering*, 10(3), 37-50. <https://doi.org/10.4236/wjnse.2020.103004>
- Hebatalrahman. (2012). The Effect of Laser Wavelength on The Microstructure Features of SS316L During Laser Irradiation *6th International Conference on Mathematics and Engineering Physics ICMEP-6* May29-31. Retrieved from <https://doi.org/10.21608/icmep.2012.29761>
- Hebatalrahman. (2014). The Microstructure Variation of Ti6Al4VELI During Excimer Laser 308nm Irradiation *9th International Conference on Electrical Engineering*, ICEENG 27-29 May. Retrieved from https://iceeng.journals.ekb.eg/article_30473.html
- Lu, X., Li, M. V., & Yang, H. (2021). Comparison of wire-arc and powder-laser additive manufacturing for IN718 superalloy: unified consideration for selecting process parameters based on volumetric energy density. *The International Journal of Advanced Manufacturing Technology*, 114, 1517-1531. <https://doi.org/10.1007/s00170-021-06990-y>
- Marchese, G., Lorusso, M., Parizia, S., Bassini, E., Lee, J. W., Calignano, F., ... & Biamino, S. (2018). Influence of heat treatments on microstructure evolution and mechanical properties of Inconel 625 processed by laser powder bed fusion. *Materials Science and Engineering: A*, 729, 64-75. <https://doi.org/10.1016/j.msea.2018.05.044>
- Moridi, A., Demir, A. G., Caprio, L., Hart, A. J., Previtali, B., & Colosimo, B. M. (2019). Deformation and failure mechanisms of Ti-6Al-4V as built by selective laser melting. *Materials Science and Engineering: A*, 768, 138456. <https://doi.org/10.1016/j.msea.2019.138456>

- Selvaganesh, S., Gajendran, P. L., Nesappan, T., & Prabhu, A. R. (2021). Comparison of clinical efficacy of diode laser and erbium, chromium: Yttrium, scandium, gallium, and garnet for implant stage 2 recovery procedure—A randomized control clinical study. *Journal of Indian Society of Periodontology*, 25(4), 335. PMID:34393405 PMCID:PMC8336765 https://doi.org/10.4103/jisp.jisp_448_20
- Wei, W., Zhang, Q., Wu, W., Cao, H., Shen, J., Fan, S., & Duan, X. (2020). Agglomeration-free nanoscale TiC reinforced titanium matrix composites achieved by in-situ laser additive manufacturing. *Scripta Materialia*, 187, 310-316. <https://doi.org/10.1016/j.scriptamat.2020.06.057>
- Xu, Y., Gong, Y., Li, P., Yang, Y., & Qi, Y. (2020). The effect of laser power on the microstructure and wear performance of IN718 superalloy fabricated by laser additive manufacturing. *The International Journal of Advanced Manufacturing Technology*, 108, 2245-2254. <https://doi.org/10.1007/s00170-020-05172-6>
- Zhao, X., Li, S., Zhang, M., Liu, Y., Sercombe, T. B., Wang, S., ... & Murr, L. E. (2016). Comparison of the microstructures and mechanical properties of Ti–6Al–4V fabricated by selective laser melting and electron beam melting. *Materials & Design*, 95, 21-31. <https://doi.org/10.1016/j.matdes.2015.12.135>
- Zhou, W., Kamata, K., Dong, M., & Nomura, N. (2021). Laser powder bed fusion additive manufacturing, microstructure evolution, and mechanical performance of carbon nanotube-decorated titanium alloy powders. *Powder Technology*, 382, 274-283. <https://doi.org/10.1016/j.powtec.2020.12.066>

Copyrights

Copyright for this article is retained by the author(s), with first publication rights granted to the journal.

This is an open-access article distributed under the terms and conditions of the Creative Commons Attribution license (<http://creativecommons.org/licenses/by/4.0/>).